Journal of Low Temperature Physics (2019) 196:42–51
https://doi.org/10.1007/s10909-018-02133-y

Prediction for Two Spatially Modulated Superfluids: ^{4}He on Fluorographene and on Hexagonal BN

Pier Luigi Silvestrelli[1,2] · Marco Nava[3] · Francesco Ancilotto[1,2] · Luciano Reatto[4]

Received: 28 June 2018 / Accepted: 15 December 2018 / Published online: 25 February 2019
© Springer Science+Business Media, LLC, part of Springer Nature 2019

Abstract

We have derived the adsorption potential of ^{4}He atoms on fluorographene (GF), on graphane and on hexagonal boron nitride (hBN) by a recently developed ab initio method that incorporates the van der Waals interaction. The stability of the commensurate $\sqrt{3} \times \sqrt{3}R30°$ phase of ^{4}He on GF and on hBN is studied by state-of-the-art quantum simulations at $T = 0$ K. With our adsorption potentials, we find that in both cases this commensurate state of ^{4}He is unstable toward a fluid state in which the ^{4}He atoms are delocalized, and not localized like in the case of ^{4}He on graphite or on graphene. In the case of GF, the present result is in qualitative agreement with the superfluid phase that was obtained using an empirical adsorption potential (Nava et al. in Phys Rev B 86:174509, 2012). This fluid state of ^{4}He on GF and on hBN is characterized by a very large density modulation. For instance, the local density changes by a factor of order 2 along the path connecting two adsorption sites. Recent experiments (Nyeki et al. in Nat Phys 13:455, 2017) have discovered a superfluid phase in the second layer ^{4}He. This is a spatially modulated superfluid that turns out to have anomalous thermal properties. This gives a strong motivation for an experimental study of monolayer ^{4}He on GF and on hBN that we predict to be a superfluid with a much stronger spatial modulation.

Keywords Helium · DFT · Superfluid · Fluorographene, hBN

✉ Luciano Reatto
luciano.reatto@mi.infn.it

1 Dipartimento di Fisica e Astronomia “Galileo Galilei” and CNISM, Università di Padova, via Marzolo 8, 35122 Padua, Italy

2 CNR-IOM Democritos, via Bonomea, 265, 34136 Trieste, Italy

3 Department of Chemistry, University of Illinois, Urbana, IL 61801, USA

4 Dipartimento di Fisica, Università degli Studi di Milano, via Celoria 16, 20133 Milan, Italy

1 Introduction

Graphene fluoride (GF) [1,2], also called fluorographene, and graphane (GH) [3,4], which have been recently obtained experimentally as chemical derivatives of graphene, are promising materials for applications in many fields, but also represent testbed substrates for investigating adsorption properties of gases and liquids. Because GF and GH have surface symmetries and compositions which are quite different from bare graphene (abbreviated Gr) and graphite, adsorbed gases will have very different properties on such substrates. Another layered material that has attracted large experimental interest is hexagonal boron nitride (hBN). hBN is an insulating isomorph of graphene, formed by alternating boron and nitrogen atoms. Also in this case, we can expect properties of the adsorption potential of atoms on hBN to be quite different from those on graphene.

The properties of a large variety of adsorbates are known in the case of interaction with Gr, but not much is known about atomic/molecular adsorption on GF, GH or hBN. Of great interest is the behavior on such substrates of light atomic adsorbates, like H_2, ^{4}He and ^{3}He, that is controlled by quantum fluctuations effects and may undergo Bose–Einstein condensation and thus display superfluid behavior. This expectation has been supported by a recent theoretical study [5] of ^{4}He adsorbed on GF and on GH based on an empirical adsorption potential [6].

The physics of quantum films has been largely based so far on detailed experimental and theoretical studies of the properties of He and H_2 on graphite substrate and, more recently, on theoretical studies for the graphene substrate [7]. In this case, the ground state of the He film on graphite is a 2D crystal commensurate with the substrate, with a $\sqrt{3} \times \sqrt{3}R30°$ structure. This ordered phase (at density $\rho = 0.0636\,\text{Å}^{-2}$) corresponds to atoms localized on second nearest-neighbor hollow sites located above hexagons of C atoms. This solid-like phase is known to be non-condensate (i.e., non-superfluid) [8]. The phase structures of ^{4}He and para-H_2 films (predicted by quantum Monte Carlo methods) on one side and both sides of graphene [9,10] have been shown to be similar to that on graphite [11–13]. A completely different behavior has been found [5] for a monolayer of ^{4}He atoms adsorbed on GF and GH: The $\sqrt{3} \times \sqrt{3}R30°$ ordered state[1] turns out to be unstable toward a fluid state, and the ground state of a monolayer of ^{4}He atoms was found to be a spatially modulated superfluid. That result is understood in the following way: The adsorption sites on GF and GH are twice as many as those on Gr or graphite, and the energy landscape of He on GF and GH substrates is characterized by a very large corrugation with narrow channels along which low potential barriers are present. Localization of ^{4}He in an adsorption site cost a large kinetic energy so that the He atoms become delocalized and visit only these channels, as though the atoms move in a multiconnected space along the bonds of a honeycomb lattice. As a result, an unprecedented strongly spatially anisotropic superfluid phase should appear, whose properties are markedly different from those of an ordinary quasi-bidimensional quantum fluid [5,6,14]. Such a novel phase has not been predicted or observed previously on any substrate. (More details on the behavior of monolayer quantum gases on graphene, graphane and fluorographene can be found in the recent

[1] In the present paper, the order of the adsorbed atoms is referred to the periodicity of the sheet of C atoms

review, and references therein, by Reatto et al [15].) The remarkable predictions made in Refs. [5] and [14] are based on accurate quantum Monte Carlo simulations. However, a basic ingredient of such simulations, i.e., the He-substrate interaction potential, was modeled using a traditional semiempirical approach [16–18], where the potential energy of a single He atom near the surface is written as a sum of pair potential interactions with different layers of the substrate for the attractive part, and a repulsive part proportional to the local electron density. These empirical potentials are known to be affected by quite large uncertainties in the empirical coefficients used to model the interaction. For this reason, we decided to investigate from first principles the interaction of He atoms with graphane (GH) and fluorographene (GF), using state-of-the-art functionals specifically designed to describe the weak VdW interactions, with the goal of providing a more accurate description of the interaction of He atoms with these surfaces. We also studied the interaction of He with a monolayer of hexagonal BN (hBN).

Numerous methods have been developed in recent years to include VdW interactions within density-functional theory (DFT), with the goal of modeling van der Waals interactions for atoms and molecules on surfaces. (For a comprehensive review on the subject, see Refs. [19], [20] and references therein.) These methods proved to be accurate in the calculation of both adsorption distances and adsorption energies, as well as the high degree of its reliability across a wide range of adsorbates.

In Sect. 2, we derive ab initio the adsorption potential of He on GF, GH and hBN. In Sect. 3, we describe our many-body computations of ^{4}He on GF and hBN and show that the ^{4}He atoms are delocalized on these substrate so that the system does not form an ordered state, but it is a highly anisotropic fluid. Our conclusions are in Sect. 4.

2 The Adsorption Potential

All calculations have been performed with the Quantum-ESPRESSO ab initio package [21]. A single He atom is considered, and we model the substrates adopting periodically repeated orthorhombic supercells, with a 4×2 structure, in the case of GF and GH, of 32 carbon atoms plus as many F or H atoms. In the case of hBN, the substrate is formed by 16 boron and 16 nitrogen atoms. The lattice constants correspond to the equilibrium state of the substrates. Repeated slabs were separated along the direction orthogonal to the surface by a vacuum region of about 24 Å to avoid significant spurious interactions due to periodic replicas. The Brillouin zone has been sampled using a $2 \times 2 \times 1$ k-point mesh. Electron–ion interactions were described using ultrasoft pseudopotentials, and the wavefunctions were expanded in a plane-wave basis set with an energy cutoff of 51 Ry.

The calculations have been performed by adopting different DFT functionals: the PBE generalized gradient approximation (GGA) functional [22], which nowadays probably represents the most popular DFT functional, the DFT-D2 [23–25] functional, where VdW corrections are implemented at a semiempirical level, and the rVV10 [26] functional (this is the revised, more efficient version of the original VV10 scheme [27]), where VdW effects are included by introducing an explicitly non-local correlation functional. rVV10 has been found to perform well in many systems and processes

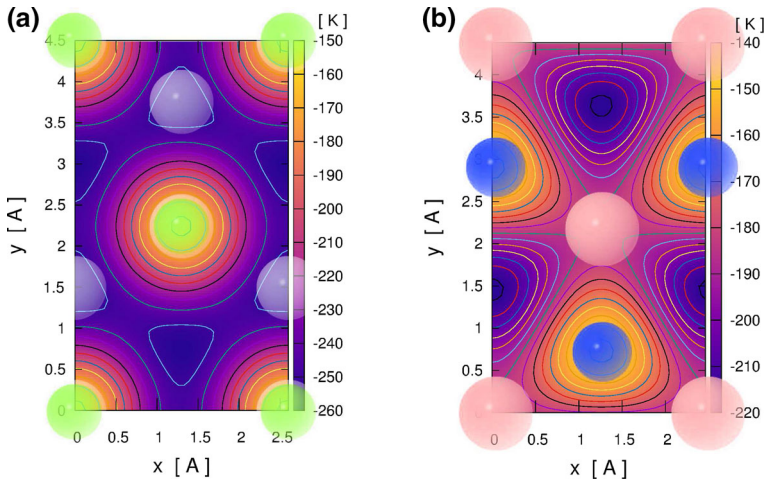

Fig. 1 Minimum potential energy map for GF (**a**) and hBN (**b**) obtained using the rVV10 functional. A top view of the atomic lattice of the substrate has been superimposed with the following coloring for the atoms. For GF: (yellow) fluorine, (gray) carbon. For hBN: (pink) boron, (blue) nitrogen (Color figure online)

where VdW effects are relevant, including several adsorption processes [26,28,29]. All the tested DFT functionals are able to well reproduce the reference structural data of graphene, graphane and fluorographene and hBN, including the "buckling displacement" in GH and GF [5].

We have calculated the equilibrium positions and adsorption energies of He on various high symmetry sites on the GF, GH and hBN substrates such as the *hollow* site, on the center of a triplet of F(H) atoms for the case of GF(GH) (or at the center of a BN ring in the case of hBN), the *top* sites, on top of a C, H, F, B or N atom, and *bridge* sites between high symmetry sites. A representation of the minimum potential energy surface of He for both GF and hBN is shown in Fig. 1. Our numerical results are summarized in Table 1. For comparison, we also show the results for the bare graphene substrate. We report the distance d of He from the substrate and the binding energy E_b of the lowest-energy configurations, which is the *hollow* site for He on graphene; the same is true for He on GF and GH, where, however, this configuration is essentially isoenergetic with that corresponding to He on *top* of a C atom (the difference in energy is smaller than 2 K), in line with the results of Ref. [5]. As a result, the relevant adsorption sites are twice as many as those occurring on Gr and graphite. The importance of properly describing VdW effects is evident: in fact, in the case of He on graphene, where reliable reference data are available [15] from experiments on graphite, the PBE functional, which does not reproduce VdW interactions, dramatically underestimate E_b and overestimate d. Among the tested VdW-corrected DFT functional, rVV10 turned out to give better performances (for instance, the semiempirical DFT-D2 approach tends to overbinding). To better characterize the adsorption of He on the different substrates, in Table 1 we also report two other energetic parameters: the "maximum corrugation", $\Delta_{\max}$, defined as the difference between the binding energy of He on top of C, H and F (which represents the less-favored configuration for

Table 1 Binding energy in the lowest-energy configuration, E_b, distance d of He from the reference plane (defined by averaging over the z coordinates of the C atoms for GF and GH and of the B and N for hBN), maximum corrugation, Δ_{max}, minimum intersite energy barrier, Δ_{min} (see text for the definitions), for He-Gr, He-GH, He-GF and for He-hBN

System	Method	E_b (K)	d(Å)	Δ_{max} (K)	Δ_{min} (K)
He-Gr	PBE	−77	3.24	17	16
He-Gr	DFT-D2	−307	2.95	56	52
He-Gr	rVV10	−298	2.96	50	47
He-Gr	Ref. [5]	−224	2.6	43	41
He-GH	PBE	−88	4.21	15	1
He-GH	DFT-D2	−209	3.77	40	7
He-GH	rVV10	−196	3.81	27	6
He-GH	Ref. [5]	−195	3.7	50	13
He-GF	PBE	−95	4.34	15	3
He-GF	DFT-D2	−287	4.07	56	12
He-GF	rVV10	−259	4.02	51	11
He-GF	Ref. [5]	−496	3.6	130	24
He-hBN	DFT-D2	−300	2.95	52	25
He-hBN	rVV10	−219	2.96	36	17

For He-Gr, the data of Ref. [5] actually refer to He on graphite

He-Gr, He-GH and He-GF, respectively) and the binding energy of the lowest-energy configuration, and the "minimum intersite energy barrier", Δ_{min}, which is given by the minimum energy barrier that the He atom must overcome to be displaced from an optimal adsorption site to another, namely from hollow to hollow for He-Gr, and from hollow to top-C for He-GH and He-GF. This latter quantity has been evaluated by monitoring the binding energy corresponding to a reaction path generated by constraining the planar x, y coordinates of the He atom and optimizing the z vertical coordinate only. In the case of hBN, Δ_{max} (Δ_{min}) correspond to the difference between the binding energy of He on top of the N(B) atom and the binding energy of the lowest-energy configuration, respectively.

As can be seen, the most striking difference between the case of He-Gr and those of He-GH and He-GF is that in He-Gr Δ_{max} and Δ_{min} are comparable, while, on the contrary, in He-GH and He-GF Δ_{min} is much smaller than Δ_{max}. This result is in qualitative agreement with the findings of Nava et al. [5], although our predicted Δ_{min} values are quantitatively even smaller than those predicted in Ref. [5]. This confirms that the adsorption potential of He on GH and GF is characterized by narrow "canyons" between adsorption sites, with a much larger anisotropy in the corrugation and a relatively low energy barrier compared to Gr and graphite. A large difference between Δ_{min} and Δ_{max} is found also for hBN so that the corrugation is larger than in the case of Gr. In addition around an adsorption site, the saddle points are 3 and not 6 as in the case of Gr.

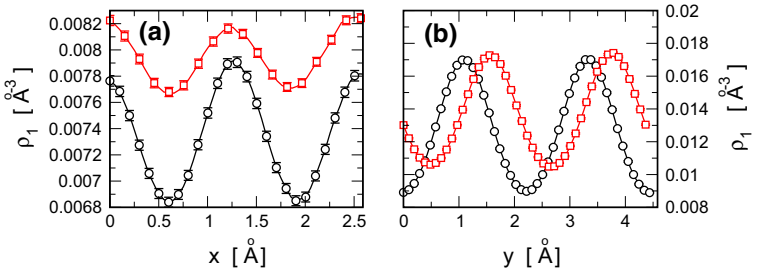

Fig. 2 Local density (normalized to the surface density of the monolayer) projected on the x direction (**a**) and the y direction (**b**) as depicted in Fig. 1 obtained from the 2-D density profile $\rho_2(x, y)$ by integrating out a variable, for $x \quad \rho_1(x) = \int \mathrm{d}y\, \rho_2(x, y)$ and in an analogous way for y. Black circles are for ^{4}He on GF and red squares for ^{4}He on hBN (Color figure online)

Besides the lowest-energy configurations for a given investigated adsorption site, we have also computed the dependence upon the normal coordinate z of the He-substrate interaction potentials above those sites. Our goal is to provide a reliable three-dimensional potential function $V_{\mathrm{He-s}}(\mathbf{r})$ which could be used for simulations of the behavior of He films on such substrates using, for instance, the phenomenological DFT approach to the properties of inhomogeneous ^{4}He systems [30] or quantum Monte Carlo simulations as we do in the present paper. We approximate the potential $V_{\mathrm{He-s}}(r)$ by using a truncated Fourier expansion over the first three stars of the two-dimensional reciprocal lattice associated with a triangular lattice with a two-atom basis (one C and one F atom in the case of GF, one B and one N atom in the case of hBN). The Fourier components can be easily obtained from the calculated z-dependence of the various symmetry sites described above.

3 Monolayer of ^{4}He on GF and hBN

The 3-D potential $V_{\mathrm{He-s}}(\mathbf{r})$ obtained from the rVV10 functional has been used in quantum Monte Carlo simulations based on the ground state path integral method [31], an unbiased $T = 0$ K method for bosons [32] with the goal of providing evidence of possible superfluid behavior of monolayer ^{4}He adsorbed on the studied substrates. The first step is to verify that a superfluid phase is not preempted by an ordered state with localized atoms as is the case of graphite and Gr. Therefore, this initial exploration focuses on the stability of the $\sqrt{3} \times \sqrt{3}R30°$ phase that could exist at density $\rho = 0.0574$ Å^{-2} for GF and $\rho = 0.0606$ Å^{-2} for hBN (the different densities arise from the slight difference of the lattice parameters of GF, hBN and graphite). We find that at such densities ^{4}He on GF and on hBN form a self-bound state with binding energies, respectively, $E_{\mathrm{b-GF}} = 1.0(1)$K and $E_{\mathrm{b-hBN}} = 0.91(9)$K per atom, the former should be compared with the value obtained in Ref. [5] with an empirical adsorption potential, $\mathrm{E}^{se}_{\mathrm{b-GF}} = 1.49(6)$K.

We have studied the structural properties at these special densities, $\rho = 0.0574$ Å^{-2} for GF and $\rho = 0.0606$ Å^{-2} for hBN. In both cases, we find a very structured density profile with modulations in the local density (Fig. 2) that have the same periodicity of

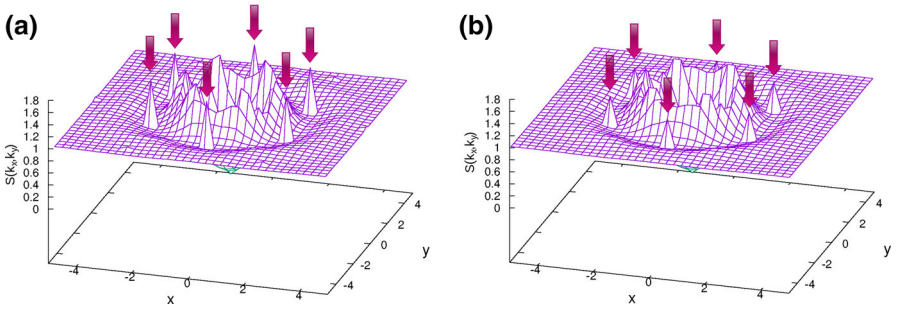

Fig. 3 Static structure factor for wave vectors relative to the adsorption surface for $N = 30$ atoms of ^{4}He on GF (**a**) and hBN (**b**). The arrows indicate the peaks corresponding to the density modulation given by the substrate (Color figure online)

the corrugation of the underlying substrate. These modulations can be quantified with the ratio Γ between the density at a peak and that at a through of the local density, for GF this value is $\Gamma_{\mathrm{GF}} = 1.91(1)$ and for hBN $\Gamma_{\mathrm{hBN}} = 1.65(1)$.

If an ordered $\sqrt{3} \times \sqrt{3}R30°$ phase were stable, the local density should have a repetition period different from that of the substrate and this is at variance from the result in Fig. 2. The absence of the $\sqrt{3} \times \sqrt{3}R30°$ order can be more clearly seen from the static structure factor, S(k). In fact, the Bragg peaks with the smallest $|\mathbf{k}| \sim 1.7\,\text{Å}^{-1}$ corresponding to a $\sqrt{3} \times \sqrt{3}R30°$ order are absent in Fig. 3, and in their place, we find a ridge in k space. Such ridge denotes short range order. The only Bragg peaks present in S(k) are those corresponding to the periodicity of the substrate. Notice the different scaling with the number N of particles of a Bragg peak (intensity proportional to N) and of a peak due to short range order (intensity independent on N). Our results for the peak intensities shown in Fig. 4 for different values of N clearly display such different scaling. The present results for GF are in qualitative agreement with those obtained in Ref. [5]

We conclude that for both substrates at low coverage of ^{4}He the $\sqrt{3} \times \sqrt{3}R30°$ ordered state is unstable and the ^{4}He is in a fluid state characterized by a very strong spatial anisotropy. Therefore, we predict the existence of two new superfluids and the explicit computation of the superfluid fraction and of the amount of BEC is a topic of further study.

4 Conclusions

We have used advanced DFT theories with VdW corrections to determine the adsorption potential for He on three substrates: GF, GH and hBN. In all three cases, the adsorption potential differs in a significant way from that for graphite and graphene due to a larger corrugation and to a strong spatial anisotropy around the adsorption sites. Our many-body quantum simulations show that the most outstanding effect is that the ordered $\sqrt{3} \times \sqrt{3}R30°$ state of ^{4}He is unstable on these substrates, and at low coverage, ^{4}He is in a fluid state characterized by a strong spatial modulation due to the substrate potential. Therefore, we predict the existence of new spatially

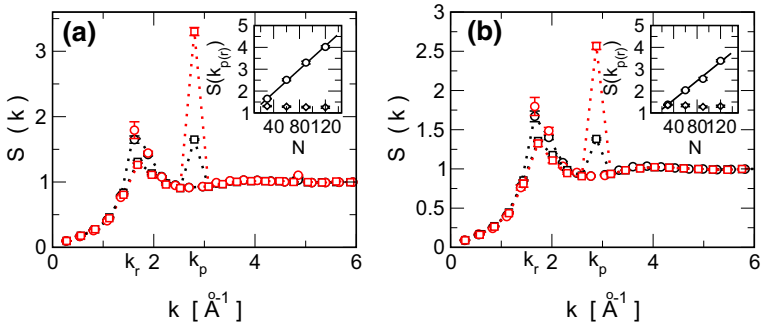

Fig. 4 Static structure factor for ^{4}He on GF (**a**) and hBN (**b**) at different system sizes: Circles refer to k_x direction and squares to k_y (as seen in Fig. 3). Black color is for $N = 30$ and red color for $N = 90$. In the insets, the intensity of the substrate modulation peaks (circles) and that of the ridge (diamonds) are plotted against the particle number N. The solid lines are linear fits to the data (Color figure online)

anisotropic superfluids. In the case of GF, the present results are in qualitative, but not in quantitative, agreement with the results of Ref. [5] based on an empirical adsorption potential.

The prediction of a spatially anisotropic superfluid is especially interesting in view of the recent results [33] on the behavior of the second layer of ^{4}He on graphite. In this case, the modulation of ^{4}He in the second layer is mainly determined by the crystalline order of the ^{4}He atoms of the first layer. A superfluid phase has been detected experimentally in the second layer with an exotic phase transition to the normal phase. Our predicted superfluid phase of ^{4}He monolayer on GF and hBN has a spatial modulation much larger than that expected for the second layer on graphite so it should be of great interest an experimental verification of our prediction.

We are not aware of experimental study of the phase diagram of ^{4}He adsorbed on hBN, while some studies have been performed for the fermionic ^{3}He [34–36]. From these NMR measurements, the authors conclude that at low temperature ^{3}He forms an ordered state and this is identified as the $\sqrt{3}\times\sqrt{3}R30°$ phase. Our study is for ^{4}He, not ^{3}He, but at first sight this conclusion seems in contradiction with our results because one might expect a stronger tendency for the atoms to be localized for the heavier ^{4}He compared to ^{3}He. A first comment is that the mentioned NMR measurements [34,35] give evidence that at a special coverage the ^{3}He atoms are in registry with those of hBN, but there is no direct evidence that this ordered phase of ^{3}He corresponds indeed to the coverage of $1/3$ of the adsorption sites, the coverage of the $\sqrt{3}\times\sqrt{3}R30°$ phase. On the basis of adsorption isotherms, this NMR special coverage can be reconciled [36] with the $\sqrt{3}\times\sqrt{3}R30°$ phase only by advocating the presence of strongly binding sites and of edge effects that are difficult to quantify. Also the presence of a liquid component [35], in addition to the solid one, over a large range of temperature and coverage is difficult to understand if the $\sqrt{3}\times\sqrt{3}R30°$ phase is indeed the lowest energy state of the monolayer as it is in the case of graphite. Our results show that the $\sqrt{3}\times\sqrt{3}R30°$ phase of ^{4}He on a monolayer of hBN is unstable, and this does not exclude that a different commensurate ordered phase might be stable at a coverage larger than 1/3. A second comment is that these measurements [34–36] are taken on

powder of hBN and it is known [37] that the adsorption properties have a significant dependence on the preparation method of the powder. In any case, the single platelets in such powders have thickness of a fraction of micron so they are formed by many layers of the basal plane. Our study is for a single layer of hBN. Our computation of the adsorption potential can be extended to the case of a multilayer hBN and it will be interesting to verify whether the instability of the $\sqrt{3} \times \sqrt{3}R30^\circ$ phase of ^{4}He on hBN remains true also for the multilayer. In addition, we should stress that our adsorption potentials are an approximation and it is difficult to quantify their accuracy. In the case of GF, an initial ordered configuration of the ^{4}He atoms becomes disordered after a small number of Monte Carlo steps so that it is unlikely that the present conclusion will be changed by the use of a more accurate adsorption potential. In the case of hBN, the relaxation of an ordered initial configuration to the disordered state is rather long so that a more accurate adsorption potential might change the balance between ordered and disordered state. In conclusion, further experimental and theoretical work seems warranted on the adsorption of the He isotopes on hBN.

Acknowledgements We thank John Saunders for bringing Ref. [34] to our attention.

References

1. R.R. Nain et al., Small **6**, 2877 (2010)
2. R. Zobril et al., Small **6**, 2885 (2010)
3. J.O. Sofo, A.S. Chaudhari, G.D. Barber, Phys. Rev. B **75**, 153401 (2007)
4. D.C. Elias et al., Science **323**, 610 (2009)
5. M. Nava, D.E. Galli, M.W. Cole, L. Reatto, Phys. Rev. B **86**, 174509 (2012)
6. L. Reatto et al., J. Phys. Conf. Ser. **400**, 012010 (2012)
7. J.G. Dash, M. Schick, O.E. Vilches, Surf. Sci. **299–300**, 405 (1994)
8. M. Buzzacchi, D.E. Galli, L. Reatto, J. Low Temp. Phys. **126**, 205 (2002)
9. Y. Kwon, D.M. Ceperley, Phys. Rev. B **85**, 224501 (2012)
10. M.C. Gordillo, Phys. Rev. B **88**, 10 (2013)
11. F.F. Abraham, J.Q. Broughton, Phys. Rev. Lett. **59**, 64 (1987)
12. M. Pierce, E. Manousakis, Phys. Rev. B **59**, 3802 (1999)
13. D. Sato et al., Phys. Rev. Lett. **109**, 235306 (2012)
14. M. Nava, D.E. Galli, M.W. Cole, L. Reatto, J. Low Temp. Phys. **171**, 699 (2013)
15. L. Reatto, D.E. Galli, M. Nava, M.W. Cole, J. Phys. Condens. Matter **25**, 443001 (2013)
16. M.J. Stott, E. Zaremba, Phys. Rev. B **22**, 1564 (1980)
17. G. Vidali, M.W. Cole, C. Schwartz, Surf. Sci. **87**, L273 (1979)
18. K.T. Tang, J.P. Toennies, J. Chem. Phys. **80**, 3726 (1984)
19. K. Berland et al., Rep. Prog. Phys. **78**, 066501 (2015)
20. J. Klimeš, A. Michaelides, J. Chem. Phys. **137**, 120901 (2012)
21. P. Giannozzi et al., J. Phys. Condens. Matter **21**, 395502 (2009)
22. J.P. Perdew, K. Burke, M. Ernzerhof, Phys. Rev. Lett. **77**, 3865 (1996)
23. S. Grimme, J. Comput. Chem. **25**, 1463 (2004)
24. S. Grimme, J. Comput. Chem. **27**, 1787 (2006)
25. S. Grimme, J. Antony, S. Ehrlich, H. Krieg, J. Chem. Phys. **132**, 154104 (2010)
26. R. Sabatini, T. Gorni, S. de Gironcoli, Phys. Rev. B **87**, 041108(R) (2013)
27. O.A. Vydrov, T. Van Voorhis, J. Chem. Phys. **133**, 244103 (2010)
28. P.L. Silvestrelli, A. Ambrosetti, Phys. Rev. B **91**, 195405 (2015)
29. P.L. Silvestrelli, A. Ambrosetti, J. Low. Temp. Phys. **185**, 183 (2016)
30. F. Ancilotto et al., Int. Rev. Phys. Chem. **36**, 621 (2017)
31. A. Sarsa, K.E. Schmidt, W.R. Magro, J. Chem. Phys. **113**, 1366 (2000)

32. M. Rossi, M. Nava, L. Reatto, D.E. Galli, J. Chem. Phys. **131**, 154108 (2009)
33. J. Nyeki et al., Nat. Phys. **13**, 455 (2017)
34. T.P. Crane, B.P. Cowan, Phys. Rev. B **62**, 11359 (2000)
35. Y. Tang, N.S. Sullivan, J. Phys. Conf. Ser. **568**, 012018 (2014)
36. T. P. Crane, in *An NMR Study of Helium-3 Adsorbed on Hexagonal Boron Nitride*, Ph.D. thesis, Royal Holloway University of London (1998)
37. R.A. Wolfson et al., Langmuir **12**, 2868 (1996)

Publisher's Note Springer Nature remains neutral with regard to jurisdictional claims in published maps and institutional affiliations.